Loss of c-Met signaling sensitizes hepatocytes to lipotoxicity and induces cholestatic liver damage by aggravating oxidative stress

Luis E. Gomez-Quiroz[a,b,1], **Daekwan Seo**[a], **Yun-Han Lee**[a,c], **Mitsuteru Kitade**[a], **Timo Gaiser**[d], **Matthew Gillen**[a], **Seung-Bum Lee**[a], **Ma Concepcion Gutierrez-Ruiz**[b], **Elizabeth A. Conner**[a], **Valentina M Factor**[a], **Snorri S. Thorgeirsson**[a], and **Jens U. Marquardt**[e,*,1]

[a] Laboratory of Experimental Carcinogenesis, Center for Cancer Research, National Cancer Institute, NIH, Bethesda, MD, USA

[b] Departamento de Ciencias de la Salud, Universidad Autonoma Metropolitana Iztapalapa, Mexico, DF, Mexico

[c] Department of Radiation Oncology, Yonsei University College of Medicine, Seoul, South Korea

[d] Institute of Pathology, University Medical Center Mannheim, Mannheim, Germany

[e] 1st Department of Medicine, University Medical Center, Johannes Gutenberg University Mainz, Langenbeckstrasse 1, 55131 Mainz, Germany

Abstract

Recent studies confirmed a critical importance of c-Met signaling for liver regeneration by modulating redox balance. Here we used liver-specific conditional knockout mice (MetKO) and a nutritional model of hepatic steatosis to address the role of c-Met in cholesterol-mediated liver toxicity.

Liver injury was assessed by histopathology and plasma enzymes levels. Global transcriptomic changes were examined by gene expression microarray, and key molecules involved in liver damage and lipid homeostasis were evaluated by Western blotting.

Loss of c-Met signaling amplified the extent of liver injury in MetKO mice fed with high-cholesterol diet for 30 days as evidenced by upregulation of liver enzymes and increased synthesis of total bile acids, aggravated inflammatory response and enhanced intrahepatic lipid deposition. Global transcriptomic changes confirmed the enrichment of networks involved in steatosis and cholestasis. In addition, signaling pathways related to glutathione and lipid metabolism, oxidative stress and mitochondria dysfunction were significantly affected by the loss of c-Met function. Mechanistically, exacerbation of oxidative stress in MetKO livers was corroborated by increased lipid and protein oxidation. Western blot analysis further revealed suppression of Erk, NF-kB and Nrf2 survival pathways and downstream target genes (e.g. cyclin D1, SOD1, gamma-GCS), as

---

[*] Corresponding author at: 1st Department of Medicine, University Medical Center, Johannes Gutenberg University Mainz, Langenbeckstrasse 1, 55131 Mainz, Germany. marquarj@uni-mainz.de (J.U. Marquardt).
[1] Shared senior authorship.

well as up-regulation of proapoptotic signaling (e.g. p53, caspase 3). Consistent with the observed steatotic and cholestatic phenotype, nuclear receptors RAR, RXR showed increased activation while expression levels of CAR, FXR and PPAR-alpha were decreased in MetKO. Collectively, our data provide evidence for the critical involvement of c-Met signaling in cholesterol and bile acids toxicity.

Keywords

c-Met; Oxidative stress; Cholestasis; Cholesterol

1. Introduction

Hepatocyte growth factor (HGF) as a major hepatic growth factor modulates a variety of liver cell types and controls a multitude of cellular processes such as proliferation, morphogenesis, survival, and motogenesis (Trusolino et al., 2010). HGF signaling is initiated by binding to its cognate receptor c-Met resulting in the activation of key signaling pathways, including phosphoinositide 3 kinase (PI3 K)/Akt, mitogen-activated protein kinases (MAPK) and extracellular signal-regulated protein kinase (ERK). In addition to these functions, we have recently demonstrated that HGF/c-Met signaling is crucial for the regulation of cellular redox status and oxidative stress. Liver-specific c-Met knockout mice (MetKO) exhibited impaired redox homeostasis due to the enhanced activation of NADPH oxidase. Under physiological conditions tissue homeostasis was maintained by a chronic activation of two critical survival transcription factors, i.e. Nuclear Factor kB (NF-kB) and Nuclear factor (erythroid-derived 2)-like 2 (Nrf2), whereby upregulation of both signaling pathways partly compensated the resulting oxidative stress in MetKO livers (Gomez-Quiroz et al., 2008; Kaposi-Novak et al., 2006).

Non-alcoholic fatty liver disease (NAFLD) is among the most common hepatic disorders worldwide with increasing frequency in the western world. NAFLD is defined by accumulation of lipids droplets in at least 5% of hepatocytes. The disease frequently progresses to non-alcoholic steatohepatitis (NASH) characterized by cell damage, inflammatory infiltration and apoptosis. Independent of etiology, the cellular and molecular mechanisms of steatosis are basically identical, and predispose the progression to advanced liver disease stages such as fibrosis, cirrhosis and/or hepatocellular carcinoma (HCC) (Dongiovanni et al., 2015; Mohamad et al., 2015).

Mari et al. (Mari et al., 2006) showed that free cholesterol may aggravate liver damage and promote the progression of fatty liver disease to NASH. Hereby, first changes were observed at the mitochondria level. Consequently, mice fed with an atherogenic diet displayed depleted mitochondrial glutathione (GSH) and increased ROS production, which rendered the animals susceptible towards subsequent adverse molecular events, e.g. by induction of tumor necrosis factor alpha (TNF-α). In addition, it has been recognized that oxidative stress may lead to cholestasis by different mechanisms such as impaired bile flow, disorganization of actin cytoskeleton, and disruption of tight-junctional structures (Masubuchi et al., 2015; Roma and Sanchez Pozzi 2008). To counteract the bile acids accumulation, hepatocytes may

activate oxidative stress-sensitive transcription factor Nrf2, as well as expression of antioxidant and phase-II and phase-III enzymes (e.g. multidrug resistance protein (MRP) 2), glutathione-related proteins (e.g. gamma-glutamylcysteine synthetase (γ-GCS) or glutathione-S-transferases) (Maher et al., 2008; Vollrath et al., 2006).

In the present work we addressed the hepatic response to an atherogenic diet (2% cholesterol, 0.5% sodium cholate) in the context of a c-Met-deficiency by using a liver specific MetKO mouse. We report that disruption of redox balance caused by c-Met inactivation plays a central role in the acceleration of cholestatic liver injury.

2. Materials and methods

2.1. Animal studies

Met$^{flx/flx}$;Alb-Cre$^{+/-}$ (MetKO) and control Met$^{wt/wt}$;Alb-Cre$^{+/-}$ (WT) mice were generated in 129SV/C57BL/6 background and genotyped as described previously (Huh et al., 2004). Mice were maintained in pathogen-free housing and cared in accordance with NIH guidelines for the care and use of laboratory animals. Eight week-old male MetKO and WT mice, twelve mice per group, were fed for 30 days with a hypercholesterolemic diet (HC) containing 2% purified cholesterol and 0.5% sodium cholate supplementation (Mari et al., 2006) (Dyets Inc). Untreated animals were fed with the regular NIH-07 diet rodent chow (Chow). All animal procedures were performed according to the protocols approved by the Animal Care and Use Committee of the National Institutes of Health and the Universidad Autonoma Metropolitana. Animals were euthanized using CO2. Terminal blood draws by axillary artery transection and liver tissue collection were performed immediately following anesthesia.

2.2. Biochemical determinations and analysis of liver function

Total bile acids (TBA) were determined in serum and liver tissue using a TBA kit (Diazyme, Poway, CA) following manufacturer's instructions. In brief, 100 mg frozen liver tissue were minced and homogenized in 1 ml ice-cold phosphate-buffered saline with protease and phosphatase inhibitors (Pierce, Rockford, IL). Samples were centrifuged at 100,000g at 4 °C and the supernatants subjected to TBA determination. Liver cholesterol content was assayed using O-phthalaldehyde according to Rudel and Morris (Rudel and Morris 1973). Caspase-3 activity was detected in homogenized liver tissue using the Caspase-3 activity fluorometric assay kit (Calbiochem, Merck KGaA, Germany) and tyriglycerides were determined by the colorimetric triglyceride quantification kit (Abcam, Cambridge, MA) following manufacturer's instructions. Serum levels of cholesterol, aspartate aminotransferase (AST), alanine transferase (ALT), bilirubin (Bil), and alkaline phosphatase (ALP) were determined by automated method using Reflovet Plus (Roche Inc).

2.3. Western blot

Total protein was isolated from liver tissue with T-Per (Pierce) extraction reagent containing 1% protease inhibitor mixture (Pierce), 100 mM sodium fluoride, 1 mM phenylmethylsulfonyl fluoride (MPSF), and 50 mM sodium orthovanadate. One hundred μg of total protein were separated on NuPAGE novex 4–20% gels (Invitrogen), transferred to

polyvinyllidene difluoride membranes (Invitrogen), and probed with antibodies listed in Supplementary Table S1 (see Supplementary material Table S1 in the online version at DOI: 10.1016/j.tox.2016.07.004). Immunoreactive bands were identified with ECL-Plus Western blotting detection reagents (GE Healthcare). Equal loading was demonstrated by probing the same membrane with anti-actin antibody (NeoMarker, Fremont, CA).

2.4. Electrophoretic mobility shift assay (EMSA)

Nuclear extracts were prepared as reported (Marquardt et al., 2012). Briefly, homogenized tissue was resuspended in Igepal CA-630 (0.58%) in 10 mM Hepes, pH 7.9, containing 10 mM KCl, 0.1 mM EDTA, 0.1 mM EGTA, 1 mM Dithithreitol (DTT), and 0.5 mM PMSF. Nuclei were pelleted in 20 mM Hepes, pH 7.9, containing 0.4 mM NaCl, 1 mM EDTA, 1 mM EGTA, 1 mM DTT, and 1 mM PMSF. After mixing for 15 min at 4 °C, samples were centrifuged at 13,000g for 5 min, and the supernatants were recovered. Protein content was assayed by BCA kit (Pierce). NF-κB and Nrf2 DNA binding activities were assayed using the EMSA "Gel shift "kit (Panomics), probing 10 μg of nuclear protein with both biotinylated NFκB-p65 consensus oligonucleotide 5′ CATCGGAAATTTCCGGAAATTTCCGGAAATTTCCGGC 3′, and Nrf2 consensus oligonucleotide 5′ GCTCTTCCGGTGCTCTTCCGGT 3′. The complexes were electrophoresed on 6% polyacrilamide native gels and transferred to a positively charged nylon membrane, 0.45 μm pore size (Schleicher and Schuell, Keene, NH). Detection was performed using the streptavidin-horseradish peroxidase conjugated. All procedure was performed according the manufacturer's instructions.

2.5. Lipid peroxidation assay

Lipid peroxidation was assayed by the production of thiobarbituric acid-reactive components (TBARS) using spectrophotometry as described by Buege and Aust (Buege and Aust 1978).

2.6. Glutathione determination by HPLC

Reduced glutathione (GSH) and oxidized glutathione (GSSG) were determined by HPLC as previously reported (Gomez-Quiroz et al., 2008).

2.7. Histology and immunohistochemistry

Formalin-fixed paraffin-embedded liver sections were stained with hematoxylin and eosin (H&E) and Oil Red O. Carbonyl modification of proteins, a key biomarker for the identification of oxidative stress, was addressed by OxyIHC oxidative stress detection kit (Millipore, Temecula, CA). After chemical derivatization of protein carbonyl groups with 2,4-dinitrophenylhydrazine (DNPH), the resulting DNP-derivatized proteins were detected by an antibody that specifically binds DNP moiety.

2.8. Microarray analysis

Micorarray analysis was performed as we described (Marquardt et al., 2012). As input, 200 ng total RNA from liver tissue were used for the *in vitro* transcription (IVT) reactions, which were incubated for 16 h at 37 °C. Hybridization, washing, detection (Cy3-streptavidin, Amersham Biosciences, GE Healthcare), and scanning were performed on an Illumina iScan

system (Illumina) using reagents and protocols supplied by the manufacturer. The biotinylated cRNA (750 ng per sample) was hybridized on Sentrix whole genome beadchips mouse Ref-8v2 for 18 h at 58 °C while rocking (5 rpm). The beadchip covers ~24,000 RefSeq transcripts. Image analysis and data extraction were performed automatically using Illumina GenomeScan Software. Gene expression values were adjusted by subtracting background noises in each spot by GenomeStudio (illumina), and normalized by quantile normalization method across all samples. Signal intensity with a detection P > 0.05 was treated as a missing value, and only genes with sufficient representation across the samples were included in further data analysis (presence in   2 replicates/group). Differentially expressed genes were identified by Bootstrap t-test with 10,000 repetitions (Neuhauser and Jockel 2006). Genes with a Bootstrap P-value   0.01 were considered significantly different. Ingenuity Pathway Analysis tool (IPA, Ingenuity Systems Inc.) was used to explore the functional relationships among the differently expressed genes. The significance of each network, function and pathway was determined by the scoring system provided by Ingenuity Pathway Analysis (IPA) tool. The microarray datasets have been deposited to Gene Expression Omnibus database (http://www.ncbi.nlm.nih.gov/geo, accession number GSE30651).

2.9. Statistical analysis

We determined statistical differences by Bootstrap t-test with 10,000 repetitions for small sample sizes. We considered values of P 0.05 statistically significant and values of P 0.01 highly significant.

3. Results

3.1. c-Met deficiency exacerbates cholestatic liver injury in mice

c-Met is implicated in a variety of metabolic processes and serves an essential stimulus for effective repair of liver damage in response to different damaging agents (Thorgeirsson 2012). To assess the role of c-Met under a stress condition, we exposed MetKO and WT mice to a 30-day course of hypercholesterolemic diet (HC) and compared the extent of liver injury in WT and MetKO mice maintained on normal chow and HC diet.

Macroscopically, the gross liver appearance of WT livers exposed to the HC diet was relatively normal. In comparison, the livers of Met-KO mice maintained on the HC diet showed an icteric dark pigmentation as well as dark-colored gallbladders indicative of cholestasis (Fig. 1A).

To assess the degree of liver damage, we first performed standard liver function tests and measured levels of aspartate transaminase (AST), alkaline phosphatase (ALP), bilirubin, total bile acids (TBA), cholesterol and triglycerides in serum and/or liver tissue. Consistently, MetKO HC diet group displayed higher levels of AST, a sensitive indicator of hepatocyte integrity, as well as ALP, a well-known marker of cholestatic damage in comparison to WT controls fed with the HC diet (Fig. 1B-C). Other markers of cholestasis significantly elevated in MetKO mice were serum bilirubin (Fig. 1D) and TBA (Fig. 1E), which were also found to be significantly increased in liver tissues of MetKO (Fig. 1H). No

differences in serum (Fig. 1F) or liver (Fig. 1I) cholesterol levels were observed between both genotypes. However, Met-KO mice maintained on the HC diet displayed a significant increase in the liver and serum triglycerides levels as compared to those in the similarly treated WT controls (Fig. 1G and J).

Consistently, a steatotic phenotype was observed by H&E staining, accompanied by a marked increase in fat accumulation in hepatocytes of MetKO-HC diet group as evidenced by Oil Red O staining (Fig. 2A,B). In addition, a stronger activation of the sterol regulatory element-binding proteins 1 (SREBP1), the major transcription factor in fatty acid synthesis (Guillou et al., 2008), was observed in livers of MetKO animals exposed to the HC diet (Fig. 2C). Histological analysis of liver sections further revealed a higher degree of infiltrating immune cells in MetKO-HC diet group (Fig. 2A, arrows). Furthermore, administration of HC diet significantly affected the expression levels of several nuclear receptors involved in the regulation of cholestasis and steatosis (Claudel et al., 2011; Moya et al., 2010; Wagner et al., 2010). Loss of c-Met signaling in the liver decreased the content of farnesoid X receptor (FXR) in response to HC administration and significantly reduced expression of constitutive androstane receptor (CAR) (Fig. 2D). HC-mediated induction of retinoic acid receptor (RAR) and downregulation of peroxisome proliferator-activated receptors alpha (PPARα) were comparable in mice of both genotypes while liver X receptor (LXR) was induced at a slightly higher degree in MetKO mice (Fig. 2C). Overall these findings indicate that genetic loss of c-Met signaling in liver amplified the extent of cholestatic injury by causing a pronounced disruption of nuclear receptors.

3.2. Transcriptomic changes induced by the atherogenic diet in MetKO mice

To dissect the molecular mechanisms underlying the cholestatic phenotype in MetKO, we performed global transcriptome profiling. In total, 1245 genes (648 upregulated and 597 downregulated) were differentially (more than 2-fold) expressed in livers from MetKO mice as compared to the corresponding WT controls when maintained on HC diet (see Supplementary material Table S2 in the online version at DOI: 10.1016/j.tox.2016.07.004). These genes were highly efficient in separating the two genotypes in an unsupervised cluster analysis (Fig. 3A). Consistent with the more advanced cholestatic injury in MetKO mice maintained on HC diet, genes involved in bile acids synthesis and excretion (Abcb6, Adh4, Cyp27a1, Cyp7ab1, and Hsd3b7) were significantly downregulated in MetKO livers. Hepatic loss of c-Met signaling also decreased expression levels of genes encoding membrane proteins including influx (Slc1a2, Slc22a1, Slc22a7, Slc29a1, Slc47a1, Slc27a5, Slc25a15, Slc17a5, Slc35e3, Slc25a45, Slc46a3, Slc6a12, Slc26a1, and Slc38a3), as well as efflux transporters (Abcb6, Abcd3, and Abcb8) of the solute carrier (SLC) family. Notably, some of the cholesterol homeostasis-related genes (Abcg5, Abcg8, Abcb11, and Abce1) were activated, potentially indicating a compensatory mechanism. In addition, many genes associated with pro- and antioxidant properties (Romo1, Pkcδ, Sod2, TNFR1, Ccs, Pkd3) as well as survival-related genes (Nfkb1, Pik3cb, Pik3c3, Egfr, Mapk9, Gstz1, Txrnd3, Aatf) were dysregulated in MetKO livers. Integrated Ingenuity Pathway Analsysis (IPA) further revealed that the major associated signaling pathways were related to mitochondria dysfunction, fatty acid, xenobiotics and GSH metabolism, bile acids biosynthesis, oxidative phosphorylation, and Nrf-2 mediated oxidative stress response (Fig. 3B). Consistently,

affected toxicological functions were involved in liver cholestasis, steatosis, inflammation, necrosis, and cell death (Fig. 3C). Thus, the altered oxidative stress response in MetKO might be responsible for the aggravated liver damage in MetKO-HC diet group.

3.3. HC administration intensifies oxidative stress in MetKO livers

To mechanistically validate the results of microarray analysis, we evaluated several parameters of oxidative stress in MetKO and control livers. In agreement with the major role of HGF/c-Met in maintaining redox balance (Clavijo-Cornejo et al., 2013; Enriquez-Cortina et al., 2013; Gomez-Quiroz et al., 2008), the ratio of reduced (GSH) to oxidized (GSSG) GSH was significantly decreased in MetKO mice even under normal condition and was further reduced by the HC diet as compared to the corresponding WT controls (Fig. 4A). MetKO mice maintained on HC diet also displayed a greater increase in lipid oxidation as measured by the rate of production of thiobarbituric acid-reactive substances (TBARS) (Fig. 4B). Immunohistochemical staining of carbonyl groups, another marker of oxidative damage was also greatly increased in MetKO liver sections from both normal chow and HC diet groups (Fig. 4C). These results demonstrate that MetKO mice experience increased oxidative stress.

3.4. Down-regulation of survival pathways in MetKO mice fed HC diet

The primary cell defense against the cytotoxic effects of oxidative stress is activation of key transcription factors involved in antioxidant response, such as Nuclear factor (erythroid-derived 2)-like 2 (Nrf2) and NF-kB, and induction of cytoprotective genes and their proteins (Gomez-Quiroz et al., 2008; Turpaev 2013). Significantly, the protein levels of Nrf2 and its major target proteins (Heme oxygenase 1 (HO1), Protein Kinase C delta (PKC-δ), NAD(P)H: Quinone Oxidoreductase 1 (NQO1) and gamma-glutamylcysteine synthetase (γ-GCS) were significantly reduced in MetKO maintained on HC diet (Chambel et al., 2015). Nrf2 down-regulation was paralleled by a coordinated activation of its repressor Keap1 while PKCδ, one of the main Nrf2 inducers (Clavijo-Cornejo et al., 2013; Niture et al., 2009), was increased, most likely as an attempt to compensate for Nrf2 down-regulation (Fig. 5A). To confirm these results we performed an EMSA analysis of Nrf2 and NF-kB. Consistently, activation of both transcription factors were significantly reduced in MetKO-HC diet group as compared to the corresponding WT group (Fig. 5B).

The increment in oxidative stress (Fig. 4) and down-regulation of two primary transcription factors responsible for cell survival under stress condition (Fig. 5A-B), were accompanied by a stronger induction of apoptosis in MetKO mice maintained on HC diet (Fig. 5C). The subsequent Western blot analysis confirmed that feeding HC diet caused a greater accumulation of pro-apoptotic proteins caspase 3 (Casp-3) and p53 in c-Met deficient mice as well as suppression of PI3 K/AKT pathway implicated in the protection against apoptosis. Of note, the downregulation of anti-apoptotic Bcl2 and induction of pro-apoptotic Bax was genotype-independent (Fig. 5D). Similarly, the Erk 1/2 activation was globally enhanced in response to the HC diet with no differences between MetKO and WT livers. However, cyclin D1 levels were preferentially increased in WT but not in MetKO-HC diet group, suggesting that cell cycle impairment may contribute to increased hepatic tissue damage (Fig. 5E).

4. Discussion

We have previously reported that genetic ablation of c-Met signaling disrupts the metabolic homeostasis of hepatocytes by a dysregulation of genes involved in lipid metabolism and stress response (Kaposi-Novak et al., 2006).

In this study we describe the protective properties of c-Met signaling against the cholesterol-induced lipotoxicity in a nutritional model of intrahepatic lipid accumulation induced by a high cholesterol diet. Interestingly, the loss of c-Met function in hepatocytes did not affect the cholesterol uptake during a 30-day course of HC diet (Fig. 1F and I). However, lipotoxic stimuli induced by the HC diet significantly aggravated liver injury in MetKO mice as evidenced by excessive lipid deposition (Fig. 2A) as well as increased levels of AST, bilirubin, and ALP (Fig. 1B,D and C), indicating that MetKO mice are more susceptible to lipotoxicity-induced cholestatic liver damage. As a consequence, macroscopic signs of cholestasis as well as profound morphological changes were visible in livers of MetKO mice (Fig. 1A).

It is well known that HGF/c-Met controls lipid metabolism in the liver. HGF administration in rats subjected to an alcoholic liquid diet markedly decreased hepatic lipid content (Tahara et al., 1999), and HGF-transgenic mice showed reduced lipid accumulation when were fed with a high-fat diet (Kosone et al., 2007). Our current data extend these findings and provide evidence that c-Met deficiency when combined with an atherogenic diet exacerbate the dysfunction in lipid metabolism. Interestingly we found a downregulation in PPARα induced by HC diet in both genotypes, but the effect was more pronounced in MetKO (Fig. 2D). Several reports provide evidence that c-Met signaling is a canonical activator of AMPK and PPARα (Vazquez-Chantada et al., 2009). Our data shows a higher decrease of PPARα in MetKO exposed to HC when compared to Chow diet, suggesting that β-oxidation can be impaired in MetKO HC mouse under atherogenic conditions.

Moreover, while TBA levels in sera of both genotypes subjected to the HC diet were significantly increased, the effect was more pronounced in the MetKO HC animals and was reflected in increased bilirubin and ALP serum levels indicating that intact c-Met signaling is an important determinant in the development of cholestatic liver disease induced by a high cholesterol diet. These results confirm recent findings advocating that HGF can improve the deleterious effects in cholestatic diseases (Giebeler et al., 2009; Song et al., 2007; Yoshikawa et al., 1998). In agreement with our findings, Li and coworkers (Li et al., 2007) reported that recombinant HGF administration to mice subjected to bile duct ligation (BDL) effectively prevented cholestasis-induced inflammation by suppressing neutrophil infiltration as well as necrosis. Further, administration of anti-HGF in BDL-treated mice induced hepatic dysfunction and hepatocyte death by necrosis and apoptosis. Giebeler (Giebeler et al., 2009) et al. also reported that c-Met deficient mice exhibited an enhanced inflammatory response after BDL mainly by neutrophils and macrophages.

The main consequences of inflammatory infiltration are the increased oxidative stress levels that cause a dramatic impairment of hepatocyte-secretory machinery thereby leading to severe disruption of the bile flow (Roma and Sanchez Pozzi 2008).

In support of this, high levels of oxidative stress markers have been consistently observed in patients with cholestatic damage. Recent reports demonstrated that 8-hydroxydeoxyguanosine was elevated in livers from patients with primary biliary cirrhosis and large bile duct obstruction (Aboutwerat et al., 2003; Kitada et al., 2001; Vendemiale et al., 2002). Additionally, experimental data revealed that CCl_4, cyclosporine A, lindane among others oxidants, induces a relevant cholestasis (Roma and Sanchez Pozzi 2008). Therefore, our data extents these findings and demonstrates that c-Met deficient hepatocytes, with high basal levels of ROS are under aggravated risk for the development of cholestasis under adverse stimuli such as lipotoxicty.

Mechanistically, c-Met signaling abrogation leads to oxidative stress by a NADPH oxidase-dependent mechanism (Clavijo-Cornejo et al., 2013), which aggravates the hepatocellular damage and liver dysfunction under the effect of major liver aggressors (Gomez-Quiroz et al., 2008; Kaposi-Novak et al., 2006; Marquardt et al., 2012; Takami et al., 2007). We here confirm that an HC diet potentiates ROS production and that c-Met deficient hepatocytes are highly susceptible to liver damage caused by this excessive ROS production. Whole transcriptome analyses further show that in addition to the known impairment of regeneration, c-Met-dependent increase in oxidative stress induces alterations in other critical signaling pathways associated to lipid, bile acid and amino acids metabolism, mitochondria dysfunction, stress response and cholestatic disease (Fig. 3).

It is well known that retention of different bile components (i.e. cholestasis) induces hepatocellular damage by the induction of apoptosis in a death-receptor dependent manner (Sodeman et al., 2000). We here demonstrate that MetKO liver overexpress proapoptotic proteins such as p53 and caspase 3 and, conversely, abrogation of Bcl2, which could be partly compensated by Mcl-1 overexpression. Interestingly, while the disruption of canonical survival pathways driven by Akt caused increased Erk1/2 activation, the severe impairment of the PI3 K/Akt pathway leading to disruption of NF-κB and Nrf2 in MetKO animals subjected to HC diet caused profound changes in the main hepatocellular adaptive response that could not be compensated.

Consistently, our data show a decrease in γ-GCS, NQO1 and HO-1 in MetKO livers, confirming the abrogation in Nrf2 pathway as a major contributing factor in the observed cholestatic phenotype. Strikingly, Nrf2 signaling in MetKO showed a diminished activation resulting in reduced protein expression as evaluated by both Western blot and EMSA, respectively (Fig. 5A,B). We could further demonstrate that these effects are associated with an increase in Keap1, suggesting a degradation of the transcription factor by proteosome 26S as an additional mechanism (Niture et al., 2010). Interestingly, the cholestatic phenotype developed despite a significant increment of PKCδ activation, which is one of the main activators of Nrf2 (Clavijo-Cornejo et al., 2013; Niture et al., 2009), potentially reflecting an adaptive response in c-Met deficient animals.

Another molecular hallmark of the pathogenesis of the lipotoxicity-induced cholestatic liver damage in MetKO HC was the altered expression of major nuclear receptors involved in lipid and bile acid homeostasis such as FXR and LXR (Calkin and Tontonoz 2012). Both molecules are known to be involved in cholesterol transport and lipogenesis (Kovanen and

Pentikainen, 2003). Consistently, FXR expression was completely abrogated in MetKO mice fed with the HC diet, supporting a causal contribution of c-Met to the cholestatic phenotype. It is known that LXR is also a potent lipogenic factor that could be inhibited by Nrf2 (Kay et al., 2011), our results show that LXR is enhanced in MetKO HC mice which could explain the increment in the activation of SREBP1 transcription factor (Fig. 2C). Even more, one of the best characterized therapeutic compounds against cholestatic disease, the ursodeoxycholic acid, is a strong stimulator of Nrf2 activation leading to detoxification, hepatocellular transport and protection against oxidative stress (Okada et al., 2009), highlighting the prominent participation of Nrf2 in the control of the homeostasis of bile acids. Further, it has been reported that the activation of SREBP1 by cholesterol in hepatocytes inhibits the transcriptional effects in CAR (Roth et al., 2008). CAR is a key regulator of xenobiotics and endobiotics known to be involved in fatty liver disease by activating fatty acid oxidation and inhibiting lipogenesis (Dong et al., 2009). Overall, the dramatic decrease of CAR expression in our model supports our findings and underlines the role of Met in this process.

5. Conclusion

In the present work we report that c-Met/HGF is essential for a coordinated response to the lipotoxic liver damage. The abrogation of c-Met signaling enhanced the oxidative stress leading to cholestatic liver damage induced by the failure to compensate the lipogenic effect of the artherogenic diet. Among the main molecular mechanisms underlying these effects is disrupted control of ROS production induced by the Nrf2 and nuclear receptor signaling. These results indicate that HGF/c-Met is involved in the protection against cholestatic liver disease and might possess therapeutic potential.

Supplementary Material

Refer to Web version on PubMed Central for supplementary material.

Acknowledgements

References

Aboutwerat A, Pemberton PW, Smith A, Burrows PC, McMahon RF, Jain SK, Warnes TW. Oxidant stress is a significant feature of primary biliary cirrhosis. Biochim. Biophys. Acta. 2003; 1637:142–150. [PubMed: 12633902]

Buege JA, Aust SD. Microsomal lipid peroxidation. Methods Enzymol. 1978; 52:302–310. [PubMed: 672633]

Calkin AC, Tontonoz P. Transcriptional integration of metabolism by the nuclear sterol-activated receptors LXR and FXR. Nat. Rev. Mol. Cell Biol. 2012; 13:213–224. [PubMed: 22414897]

Chambel SS, Santos-Goncalves A, Duarte TL. The dual role of Nrf2 in nonalcoholic fatty liver disease: regulation of antioxidant defenses and hepatic lipid metabolism. Biomed Res Int. 2015; 2015:597–607.

Claudel T, Zollner G, Wagner M, Trauner M. Role of nuclear receptors for bile acid metabolism, bile secretion, cholestasis, and gallstone disease. Biochim. Biophys. Acta. 2011; 1812:867–878. [PubMed: 21194565]

Clavijo-Cornejo D, Enriquez-Cortina C, Lopez-Reyes A, Dominguez-Perez M, Nuno N, Dominguez-Meraz M, Bucio L, Souza V, Factor VM, Thorgeirsson SS, Gutierrez-Ruiz MC, Gomez-Quiroz LE. Biphasic regulation of the NADPH oxidase by HGF/c-Met signaling pathway in primary mouse hepatocytes. Biochimie. 2013; 95:1177–1178. [PubMed: 23333744]

Dong B, Saha PK, Huang W, Chen W, Abu-Elheiga LA, Waki SJ, Stevens RD, Iikayeva O, Newgard CB, Chan L, Moore DD. Activation of nuclear receptor CAR ameliorates diabetes and fatty liver disease. Proc. Natl. Acad. Sci. U. S. A. 2009; 106:18831–18836. [PubMed: 19850873]

Dongiovanni P, Romeo S, Valenti L. Genetic factors in the pathogenesis of nonalcoholic fatty liver and steatohepatitis. Biomed. Res. Int. 2015; 2015:460190. [PubMed: 26273621]

Enriquez-Cortina C, Almonte-Becerril M, Clavijo-Cornejo D, Palestino-Dominguez M, Bello-Monroy O, Nuno N, Lopez A, Bucio L, Souza V, Hernandez-Pando R, Munoz L, Gutierrez-Ruiz MC, Gomez-Quiroz LE. Hepatocyte growth factor protects against isoniazid/rifampicin-induced oxidative liver damage. Toxicol. Sci. 2013; 135:26–36. [PubMed: 23764483]

Giebeler A, Boekschoten MV, Klein C, Borowiak M, Birchmeier C, Gassler N, Wasmuth HE, Muller M, Trautwein C, Streetz KL. c-Met confers protection against chronic liver tissue damage and fibrosis progression after bile duct ligation in mice. Gastroenterology. 2009; 137:297–308. 308, e291–294. [PubMed: 19208365]

Gomez-Quiroz LE, Factor VM, Kaposi-Novak P, Coulouarn C, Conner EA, Thorgeirsson SS. Hepatocyte-specific c-Met deletion disrupts redox homeostasis and sensitizes to Fas-mediated apoptosis. J. Biol. Chem. 2008; 283:14581–14589. [PubMed: 18348981]

Guillou H, Martin PG, Pineau T. Transcriptional regulation of hepatic fatty acid metabolism. Subcell. Biochem. 2008; 49:3–47. [PubMed: 18751906]

Huh CG, Factor VM, Sanchez A, Uchida K, Conner EA, Thorgeirsson SS. Hepatocyte growth factor/c-met signaling pathway is required for efficient liver regeneration and repair. Proc. Natl. Acad. Sci. U. S. A. 2004; 101:4477–4482. [PubMed: 15070743]

Kaposi-Novak P, Lee JS, Gomez-Quiroz L, Coulouarn C, Factor VM, Thorgeirsson SS. Met-regulated expression signature defines a subset of human hepatocellular carcinomas with poor prognosis and aggressive phenotype. J. Clin. Invest. 2006; 116:1582–1595. [PubMed: 16710476]

Kay HY, Kim WD, Hwang SJ, Choi HS, Gilroy RK, Wan YJ, Kim SG. Nrf2 inhibits LXRalpha-dependent hepatic lipogenesis by competing with FXR for acetylase binding. Antioxid. Redox Signaling. 2011; 15:2135–2146.

Kitada T, Seki S, Iwai S, Yamada T, Sakaguchi H, Wakasa K. In situ detection of oxidative DNA damage, 8-hydroxydeoxyguanosine, in chronic human liver disease. J. Hepatol. 2001; 35:613–618. [PubMed: 11690707]

Kosone T, Takagi H, Horiguchi N, Ariyama Y, Otsuka T, Sohara N, Kakizaki S, Sato K, Mori M. HGF ameliorates a high-fat diet-induced fatty liver. Am. J. Physiol. Gastrointest. Liver Physiol. 2007; 293:G204–210. [PubMed: 17395903]

Kovanen TT, Pentikainen MO. Pharmacological evidence for role of liver X receptors in atheroprotection. FEBS Lett. 2003; 536:3–5. [PubMed: 12586328]

Li Z, Mizuno S, Nakamura T. Antinecrotic and antiapoptotic effects of hepatocyte growth factor on cholestatic hepatitis in a mouse model of bile-obstructive diseases. Am. J. Physiol. Gastrointest. Liver Physiol. 2007; 292:G639–646. [PubMed: 17068118]

Maher JM, Aleksunes LM, Dieter MZ, Tanaka Y, Peters JM, Manautou JE, Klaassen CD. Nrf2- and PPAR alpha-mediated regulation of hepatic Mrp transporters after exposure to perfluorooctanoic acid and perfluorodecanoic acid. Toxicol. Sci. 2008; 106:319–328. [PubMed: 18757529]

Mari M, Caballero F, Colell A, Morales A, Caballeria J, Fernandez A, Enrich C, Fernandez-Checa JC, Garcia-Ruiz C. Mitochondrial free cholesterol loading sensitizes to TNF- and Fas-mediated steatohepatitis. Cell Metab. 2006; 4:185–198. [PubMed: 16950136]

Marquardt JU, Seo D, Gomez-Quiroz LE, Uchida K, Gillen MC, Kitade M, Kaposi-Novak P, Conner EA, Factor VM, Thorgeirsson SS. Loss of c-Met accelerates development of liver fibrosis in

response to CCl(4) exposure through deregulation of multiple molecular pathways. Biochim. Biophys. Acta. 2012

Masubuchi N, Sugihara M, Sugita T, Amano K, Nakano M, Matsuura T. Oxidative stress markers, secondary bile acids and sulfated bile acids classify the clinical liver injury type: promising diagnostic biomarkers for cholestasis. Chem. Biol. Interact. 2015

Mohamad B, Shah V, Onyshchenko M, Elshamy M, Aucejo F, Lopez R, Hanouneh IA, Alhaddad R, Alkhouri N. Characterization of hepatocellular carcinoma (HCC) in non-alcoholic fatty liver disease (NAFLD) patients without cirrhosis. Hepatol. Int. 2015

Moya M, Gomez-Lechon MJ, Castell JV, Jover R. Enhanced steatosis by nuclear receptor ligands: a study in cultured human hepatocytes and hepatoma cells with a characterized nuclear receptor expression profile. Chem. Biol. Interact. 2010; 184:376–387. [PubMed: 20079722]

Neuhauser M, Jockel KH. A bootstrap test for the analysis of microarray experiments with a very small number of replications. Appl. Bioinf. 2006; 5:173–179.

Niture SK, Jain AK, Jaiswal AK. Antioxidant-induced modification of INrf2 cysteine 151 and PKC-delta-mediated phosphorylation of Nrf2 serine 40 are both required for stabilization and nuclear translocation of Nrf2 and increased drug resistance. J. Cell Sci. 2009; 122:4452–4464. [PubMed: 19920073]

Niture SK, Kaspar JW, Shen J, Jaiswal AK. Nrf2 signaling and cell survival. Toxicol. Appl. Pharmacol. 2010; 244:37–42. [PubMed: 19538984]

Okada K, Shoda J, Taguchi K, Maher JM, Ishizaki K, Inoue Y, Ohtsuki M, Goto N, Sugimoto H, Utsunomiya H, Oda K, Warabi E, Ishii T, Yamamoto M. Nrf2 counteracts cholestatic liver injury via stimulation of hepatic defense systems. Biochem. Biophys. Res. Commun. 2009; 389:431–436. [PubMed: 19732748]

Roma MG, Sanchez Pozzi EJ. Oxidative stress: a radical way to stop making bile. Ann. Hepatol. 2008; 7:16–33. [PubMed: 18376363]

Roth A, Looser R, Kaufmann M, Meyer UA. Sterol regulatory element binding protein 1 interacts with pregnane X receptor and constitutive androstane receptor and represses their target genes. Pharmacogenet. Genomics. 2008; 18:325–337. [PubMed: 18334917]

Rudel LL, Morris MD. Determination of cholesterol using o-phthalaldehyde. J. Lipid Res. 1973; 14:364–366. [PubMed: 14580182]

Sodeman T, Bronk SF, Roberts PJ, Miyoshi H, Gores GJ. Bile salts mediate hepatocyte apoptosis by increasing cell surface trafficking of Fas. Am. J. Physiol. Gastrointest. Liver Physiol. 2000; 278:G992–999. [PubMed: 10859230]

Song KH, Ellis E, Strom S, Chiang JY. Hepatocyte growth factor signaling pathway inhibits cholesterol 7alpha-hydroxylase and bile acid synthesis in human hepatocytes. Hepatology. 2007; 46:1993–2002. [PubMed: 17924446]

Tahara M, Matsumoto K, Nukiwa T, Nakamura T. Hepatocyte growth factor leads to recovery from alcohol-induced fatty liver in rats. J. Clin. Invest. 1999; 103:313–320. [PubMed: 9927491]

Takami T, Kaposi-Novak P, Uchida K, Gomez-Quiroz LE, Conner EA, Factor VM, Thorgeirsson SS. Loss of hepatocyte growth factor/c-Met signaling pathway accelerates early stages of N-nitrosodiethylamine induced hepatocarcinogenesis. Cancer Res. 2007; 67:9844–9851. [PubMed: 17942915]

Thorgeirsson SS. The central role of the c-Met pathway in rebuilding the liver. Gut. 2012; 61:1105–1106. [PubMed: 22387525]

Trusolino L, Bertotti A, Comoglio PM. MET signalling: principles and functions in development, organ regeneration and cancer. Nat. Rev. Mol. Cell Biol. 2010; 11(12):834–848. [PubMed: 21102609]

Turpaev KT. Keap1-Nrf2 signaling pathway: mechanisms of regulation and role in protection of cells against toxicity caused by xenobiotics and electrophiles. Biochemistry (Mosc). 2013; 78:111–126. [PubMed: 23581983]

Vazquez-Chantada M, Ariz U, Varela-Rey M, Embade N, Martinez-Lopez N, Fernandez-Ramos D, Gomez-Santos L, Lamas S, Lu SC, Martinez-Chantar ML, Mato JM. Evidence for LKB1/AMP-activated protein kinase/ endothelial nitric oxide synthase cascade regulated by hepatocyte growth

factor, S-adenosylmethionine, and nitric oxide in hepatocyte proliferation. Hepatology. 2009; 49:608–617. [PubMed: 19177591]

Vendemiale G, Grattagliano I, Lupo L, Memeo V, Altomare E. Hepatic oxidative alterations in patients with extra-hepatic cholestasis. Effect of surgical drainage. J. Hepatol. 2002; 37:601–605. [PubMed: 12399225]

Vollrath V, Wielandt AM, Iruretagoyena M, Chianale J. Role of Nrf2 in the regulation of the Mrp2 (ABCC2) gene. Biochem. J. 2006; 395:599–609. [PubMed: 16426233]

Wagner M, Zollner G, Trauner M. Nuclear receptor regulation of the adaptive response of bile acid transporters in cholestasis. Semin. Liver Dis. 2010; 30:160–177. [PubMed: 20422498]

Yoshikawa A, Kaido T, Seto S, Yamaoka S, Sato M, Ishii T, Imamura M. Hepatocyte growth factor promotes liver regeneration with prompt improvement of hyperbilirubinemia in hepatectomized cholestatic rats. J. Surg. Res. 1998; 78:54–59. [PubMed: 9733618]
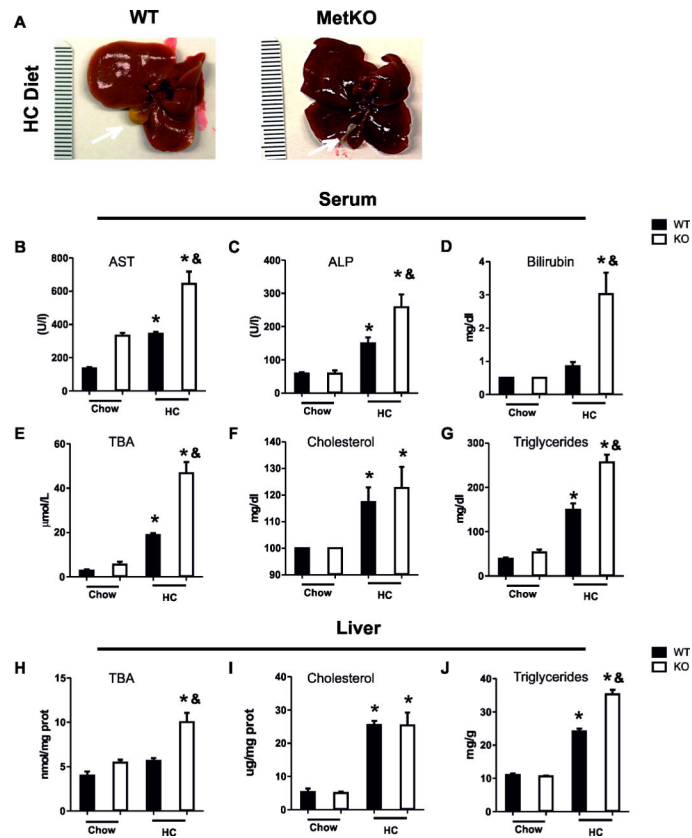
Fig. 1.
MetKO mice fed the high-cholesterol diet develop liver damage. A: Gross liver appearance. B-J: Biochemical evaluation of liver damage. Serum levels of aspartate aminotransferase (AST) (B); alkaline phosphatase (ALP) (C); total bilirubin (D); total bile acids (TBA) (E); cholesterol (F); triglycerides (G); and liver levels of TBA (H); cholesterol (I);and triglycerides (J). Each column represents mean SEM of at least six animals. $*p < 0.05$ vs WT chow diet; $\&p < 0.05$ vs WT high-cholesterol (HC) diet.
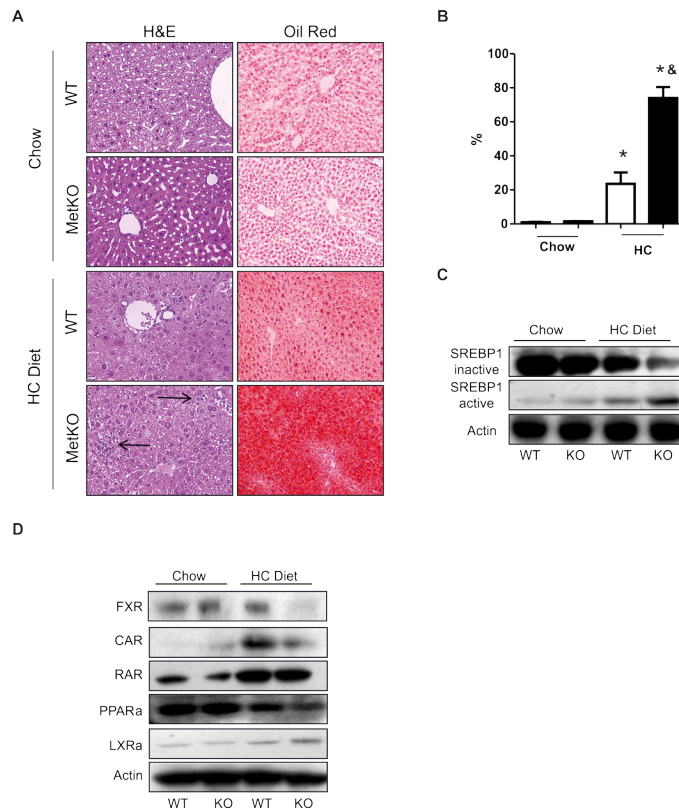
Fig. 2.
High-cholesterol diet induces steatohepatitis and affects major nuclear receptors and lipogenic-related factors. A: hematoxylin & eosin and Oil red O staining on paraffin liver sections from MetKO or WT mice fed the high-cholesterol (HC) diet or control chow diet. Original magnification, X200. Arrows show inflammatory infiltration. Images are representatives of at least four animals for each group. B: Quantification of fat accumulation. * $p < 0.05$ vs WT chow diet; & $p < 0.05$ vs WT high-cholesterol (HC) diet. C: Activation of sterol regulatory element-binding protein 1 (SREBP1). D: Western blots of nuclear receptors related to lipid and bile acids metabolism: Farnesoid X Receptor (FXR), Constitutive androstane receptor (CAR), Retinoid Acid Receptor (RAR), Peroxisome proliferator-activated receptor alpha (PPAR-α), and Liver X Receptor alpha (LXRα). Images are representative of at least three independent experiments. Actin was used as a loading control.

A

597 genes

648 genes

WT
MetKO

C

Top toxicological functions

#	Pathway	pValue
1	Liver Cholestasis	1.14E-07 – 2.57E-01
2	Liver Steatosis	3.24E-04 – 3.61E-01
3	Renal Necrosis	1.75E-03 – 5.9E-01
4	Liver Hepatomegaly	3.32E-03 – 6.14E-01
5	Liver Inflammation	3.32E-03 – 3.93E-02
6	Liver Necrosis/cell death	3.32E-03 – 5.38E-01
7	Cardiac Infarction	3.35E-03 – 4.24E-01
8	Liver Adhesion	3.35E-03
9	Cardiac Hypertrophy	8.90E-03 – 1.00E 01
10	Liver Damage	9.98E-03- 1.70E-01

B

Top signaling pathways

#	Pathway	pValue	Ratio
1	Mitochondria Dysfunction	4.68E -10	29/175
2	Tryptophan Metabolism	1.03E -07	26/246
3	Tyrosine Metabolism	2.22E -07	19/209
4	Fatty Acid Metabolism	8.79E -07	23/119
5	Metabolism of Xenobiotics	4.00E -06	21/200
6	Ubiquinone Biosynthesis	4.51E -06	16/119
7	Oxidative Phosphorylation	5.02E -06	24/165
8	Arachidonic Acid Metabolism	3.33E -05	21/218
9	Bile Acid Biosynthesis	4.55E -05	12/107
10	GSH Metabolism	7.17E -05	13/98
11	Acute Phase Response signaling	1.54E -05	20/178
12	Nrf2-mediated oxidative stress response	1.62E -02	18/192

Fig. 3.

Microarray analyses. A: Unsupervised hierarchical cluster analyses of liver tissue from MetKO mice or WT fed with the high-cholesterol (HC) diet for 30 days. A total of 1245 differentially expressed genes were identified using bootstrap t-test with 10,000 repetitions (p-value 0.01). B: Top signaling pathways in livers from MetKO mice fed with HC or normal chow diets as determined by IPA analysis. C: Top toxicological functions affected in MetKO mice fed with HC diet as determined by IPA analysis.
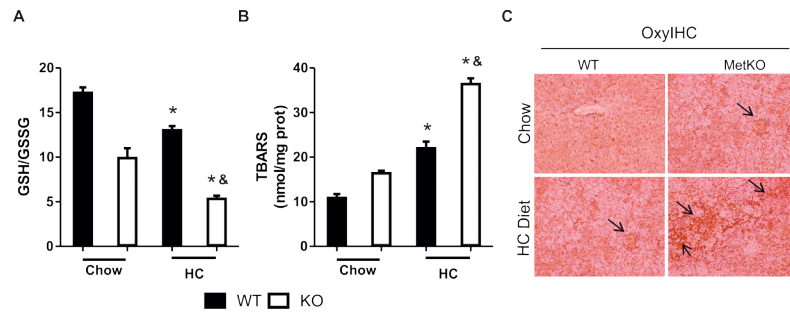
Fig. 4.
High-cholesterol diet exacerbates oxidative stress in MetKO mice. A: Glutathione ratio determined by HPLC as described in Materials and Methods. B: Lipid peroxidation. TBARS, thiobarbituric acid reactive substances. Each column represents mean ± SEM of at least four independent experiments. $*p < 0.05$ vs WT chow diet; $\&p < 0.05$ vs WT high-cholesterol (HC) diet. C: Protein oxidation, carbonyl modification was determined by IHC using OxyIHC kit as described in Materials and Methods. Original magnification, X200. Arrows show oxidized protein areas. Images are representatives of at least four animals for each group.
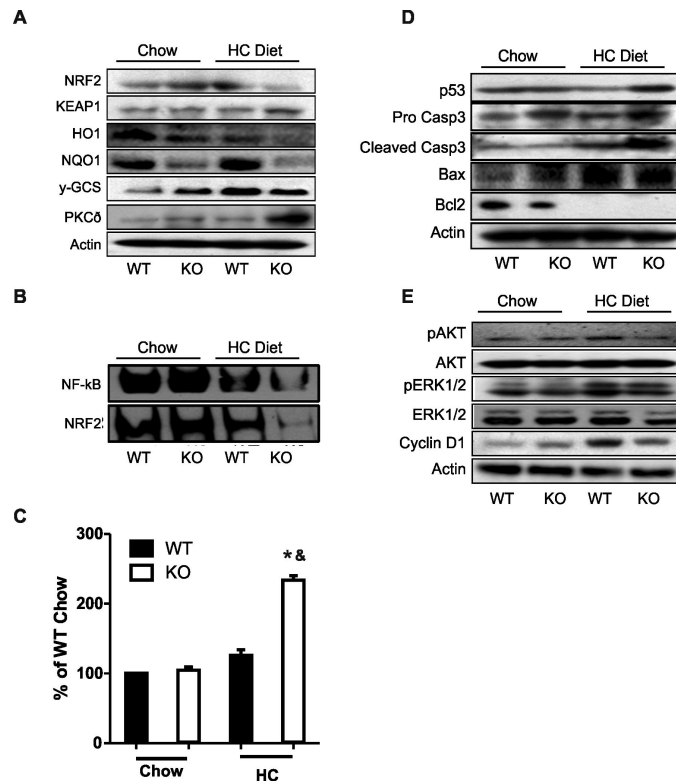
Fig. 5.
High-cholesterol diet affects cell survival pathways and induces apoptosis in MetKO mice. A: Western blotting of Nrf2-related proteins including Nuclear Factor (erythroid-derived 2)-like 2 (NRF2), NRF2 inhibitor Kelch-like ECH-associated protein 1 (KEAP1); Heme oxygenase 1(HO1); NAD(P)H: Quinone Oxidoreductase 1: (NQO1); gamma-glutamylcysteine synthetase (γ-GCS); Protein Kinase C delta (PKC-δ). B: EMSA analysis of Nuclear Factor kB (NF-kB) and NRF2 transcription factors. C: Caspase 3 activity. Each column represents mean ± SEM of at least four independent experiments. $*p < 0.05$ vs WT chow diet; $\&p < 0.05$ vs WT high-cholesterol (HC) diet. D: Apoptosis-related proteins p53, Caspase 3 (Casp3), Bax, and Bcl2. E: Survival-related proteins Akt, Erk1/2 and Cyclin D1. Images are representative of at least three independent experiments. For Western blotting (A, D and E) actin was used as a loading control.